9-5-2007

Ovarian Cancer G Protein–Coupled Receptor 1, a New Metastasis Suppressor Gene in Prostate Cancer

Lisam Shanjukumar Singh
Indiana University

Michael Berk
Cleveland Clinic

Rhonda Oates
Cleveland Clinic

Zhenwei Zhao
Indiana University

Haiyan Tan
Cleveland Clinic

Publisher's Statement

"This is a pre-copyedited, author-produced PDF of an article accepted for publication in Journal of the National Cancer Institute following peer review. The version of record Singh, L. S.; Berk, M.; Oates, R.; Zhao, Z.; Tan, H.; Jiang, Y.; Zhou, A.; Kirmani, K.; Steinmetz, R.; Lindner, D.; Xu, Y., Ovarian Cancer G Protein–Coupled Receptor 1, a New Metastasis Suppressor Gene in Prostate Cancer. JNCI: Journal of the National Cancer Institute 2007, 99 (17), 1313-1327.] is available online at: https://academic.oup.com/jnci/article/99/17/1313/2522257

Authors
Lisam Shanjukumar Singh, Michael Berk, Rhonda Oates, Zhenwen Zhao, Haiyan Tan, Ying Jiang, Aimin Zhou, Kashif Kirmani, Rosemary Steinmetz, Daniel Lindner, and Yan Xu

Ovarian Cancer G Protein–Coupled Receptor 1, a New Metastasis Suppressor Gene in Prostate Cancer

Lisam Shanjukumar Singh, Michael Berk, Rhonda Oates, Zhenwen Zhao, Haiyan Tan, Ying Jiang, Aimin Zhou, Kashif Kirmani, Rosemary Steinmetz, Daniel Lindner, Yan Xu

Background Metastasis is a process by which tumors spread from primary organs to other sites in the body and is the major cause of death for cancer patients. The ovarian cancer G protein–coupled receptor 1 (OGR1) gene has been shown to be expressed at lower levels in metastatic compared with primary prostate cancer tissues.

Methods We used an orthotopic mouse metastasis model, in which we injected PC3 metastatic human prostate cancer cells stably transfected with empty vector (vector-PC3) or OGR1-expressing vector (OGR1-PC3) into the prostate lobes of athymic or NOD/SCID mice (n = 3–8 mice per group). Migration of PC3 cells transiently transfected with vector control or with OGR1- or GPR4 (a G protein–coupled receptor with the highest homology to OGR1)-expressing vectors was measured in vitro by Boyden chamber assays. G protein alpha–inhibitory subunit 1 ($G\alpha_{i1}$) expression after treatment with pertussis toxin (PTX) was measured using immunoblotting analysis. The inhibitory factor present in the conditioned medium was extracted using organic solvents and analyzed by mass spectrometry.

Results In vivo, all 26 mice carrying tumors that were derived from vector-PC3 cells developed prostate cancer metastases (mean = 100%, 95% confidence interval [CI] = 83.97% to 100%) but few (4 of 32) mice carrying tumors derived from OGR1-expressing PC3 cells (mean = 12.50%, 95% CI = 4.08% to 29.93%) developed metastases. However, exogenous OGR1 overexpression had no effect on primary prostate tumor growth in vivo. In vitro, expression of OGR1, but not GPR4, inhibited cell migration (mean percentage of cells migrated, 30.2% versus 100%, difference = 69.8%, 95% CI = 63.0% to 75.9%; $P<.001$) via increased expression of $G\alpha_{i1}$ and the secretion of a chloroform/methanol–extractable heat-insensitive factor into the conditioned medium through a PTX-sensitive pathway.

Conclusion OGR1 is a novel metastasis suppressor gene for prostate cancer. OGR1's constitutive activity via $G\alpha_i$ contributes to its inhibitory effect on cell migration in vitro.

J Natl Cancer Inst 2007;99:1313–27

Approximately 1.4 million new cancers were diagnosed, and more than 564 000 deaths from cancer were expected, in the United States in 2006 (1). The majority of these cancer-related deaths will be due to tumor metastasis rather than to the primary tumors. Thus, the major clinical challenge is to combat systemic metastatic disease.

Unlike tumor suppressor genes, such as p53 and Rb, metastasis suppressor genes reduce the metastatic propensity of cancer cell lines without substantially affecting their tumorigenesis in vivo (2–4). Well-defined metastasis suppressor genes include NM23, MKK4, KAI1, BRMS1, KiSS1, RHOGDI2, CRSP3, and VDUP1 (2,5,6). Metastasis suppressor genes operate at different levels in the metastatic process (2,3) through mechanisms that involve mitogen-activated protein (MAP) kinase (ERK, p38, and JNK kinases) regulation, integrin interaction, epidermal growth factor desensitization, Gap junction communication, modulation of G protein–coupled receptors or G proteins; they can also function as coactivators of transcription and inhibitors of thioredoxin (2,3,5). Targeting metastasis suppressor genes has high therapeutic potential. Although there are many steps in metastasis, blocking only one of these steps may potentially inhibit or prevent metastasis. Moreover, unlike classical tumor suppressor genes, most metastasis suppressor genes are not mutated in tumor tissues but instead their expression is suppressed by promoter methylation and/or other mechanisms. Thus, restoring metastasis suppressor gene expression may be sufficient to suppress tumor metastasis (5,7).

CONTEXT AND CAVEATS

Prior knowledge

Tumor metastasis is a major cause of death among cancer patients. The expression of ovarian cancer G protein–coupled receptor 1 (OGR1) is higher in primary prostate tumors than metastases.

Study design

Mouse models of prostate cancer metastasis and in vitro migration assays using control human prostate cancer cells and those engineered to overexpress OGR1.

Contributions

Cells overexpressing OGR1 formed fewer metastases in the mouse models and migrated more slowly in vitro than control cells.

Implications

OGR1 acts as a metastasis suppressor gene in prostate cancer.

Study limitations

Only one prostate cancer cell line was used in the mouse models. In these models, this cell line did not metastasize to bone, which is one of the most common sites of metastasis in prostate cancer as well as other types of cancer. Thus, how OGR1 might affect metastasis to bone is unknown, as is the application of these findings to human prostate cancer.

Identifying prostate cancer–related metastasis suppressor genes and their mechanisms of action is important for the development of novel strategies for the prevention and treatment of metastatic prostate tumors. An estimated 234 460 new cases and 27 350 deaths from prostate cancer were expected in the United States in 2006 (1). With the introduction of the prostate-specific antigen (PSA) screening test, approximately 75% of prostate cancers are detected when the disease is clinically confined to the prostate. However, in many patients, the cancer often progresses to an androgen-independent metastatic stage for which few treatment options are available. Several metastasis suppressor genes have been identified in prostate cancer, including CD44, NM23, MKK4, and KAI1 (8).

G proteins and G protein–coupled receptors have important roles in prostate cancer (9–11) and in other pathologic processes. Of the 100 leading pharmaceutical products developed in 2000, 39 act through a G protein–coupled receptor–mediated mechanism, underlining the importance of G protein–coupled receptors as important pharmaceutical targets (12). We have previously cloned OGR1, a G protein–coupled receptor from the HEY human ovarian cancer cell line (13). OGR1 and related subfamily members GPR4, G2A, and TDAG8 mediate the functions of several lysophospholipids, including sphingosylphosphorylcholine (SPC), lysophosphatidylcholine (LPC), and psychosine (14–18), which include endothelial barrier function, endothelial cell proliferation, migration, and tube formation, T cell migration, glucocorticoid-induced thymocyte apoptosis, and globoid cell formation.

In addition, all members of the OGR1 subfamily exhibit proton-sensing properties (19,20). Using small hairpin RNA to inhibit expression of GPR4 followed by replenishment with mutant GPR4, we have shown that endogenous GPR4 mediates the proliferation, migration, and tube formation effects of SPC. In addition, unlike earlier studies in HEK293 cells, for which GPR4 overexpression resulted in increased cAMP production in response to changes in cellular pH (19), we have shown (15) that, in endothelial cells, endogenous GPR4 does not increase cAMP production in response to pH changes.

Although more extensive work is warranted to further clarify these apparently conflicting findings related to pH and lipid regulators and/or modulators, OGR1 and related G protein–coupled receptors also possess constitutive activities that do not require ligand binding and are not affected by pH changes (15). Many G protein–coupled receptors undergo a spontaneous switch between their inactive and active states (induced or stabilized by the agonist). When these receptors undergo agonist-independent stabilization of the active state, they become constitutively active, which results in an increase in basal G protein activity. Constitutive activity is observed in numerous G protein–coupled receptors (21) and can be achieved through various mechanisms (12,21–23).

LaTulippe et al. (24) have conducted a comprehensive gene expression analysis of prostate cancer using oligonucleotide arrays with more than 63 000 probe sets to identify genes and expressed sequences with substantial differential expression between non-recurrent primary prostate cancers and metastatic prostate cancers. Interestingly, among the top 100 differentially expressed genes that were identified in this study, OGR1 expression was shown to be fivefold lower in tumor metastases than primary tumors (24).

In this study, we investigated the role of OGR1 in prostate cancer metastasis using an orthotopic model in athymic (nu/nu) and non-obese diabetic/severe combined immunodeficiency (NOD/SCID) mice. We also investigated the effects of OGR1 expression on metastatic prostate cancer cell migration in vitro and the mechanisms underlying these effects using stable PC3 prostate cancer cell clones.

Materials and Methods

Materials

Male athymic mice (n = 26, 5–7 weeks old; nu/nu) were obtained from Charles River Laboratories (Wilmington, MA). Male NOD/SCID mice (n = 32, 5–7 weeks old) were obtained either from Jackson Laboratory (Bar Harbor, ME) or from Dr Karen Pollok at the Indiana University School of Medicine (Indianapolis, IN). Mice were housed at the Cleveland Clinic's Laboratory Animal Resource Unit (Cleveland, OH) or at the Laboratory Animal Resource Center at the Indiana University School of Medicine. Immunohistochemistry kits were obtained from Vector Laboratories (Burlingame, CA). G protein alpha–inhibitory subunit ($G\alpha_{i1}$) dominant-negative cDNAs were purchased from the University of Missouri's UMR cDNA Resource Center (Rolla, MO). Rabbit polyclonal anti-$G\alpha_{i1}$ antibody was from Santa Cruz Biotechnology (Santa Cruz, CA). Mouse monoclonal anti-BrdU antibody and methylthiazolyldiphenyl-tetrazolium bromide (MTT) were obtained from Sigma (St Louis, MO), rabbit polyclonal anti-OGR1 antibody was purchased from LifeSpan BioSciences (Seattle, WA), and rat monoclonal anti-mouse CD49b/Pan-NK-cells antibody was purchased from BD Biosciences (San Jose, CA).

Cell Culture

The androgen-independent metastatic human prostate cancer cell line PC3 and the human embryonic kidney 293T (HEK293T) cell

line were purchased from American Type Culture Collection (Manassas, VA). The immortalized human microvascular endothelial cell line-1 (HMEC-1) was from the Centers for Disease Control and Prevention (Atlanta, GA). PC3 and HMEC-1 cells were cultured in RPMI-1640. C4-2 and DU145 human prostate cancer cell lines (obtained from Dr Warren Heston at the Cleveland Clinic), and HEK293T cells were cultured in Dulbecco's modified Eagle medium. Media were supplemented with 10% fetal bovine serum (FBS), 100 units/mL penicillin–streptomycin, and 2 mM glutamine. Cells were maintained in a humidified 5% CO_2 atmosphere at 37 °C.

Plasmid Construction

The pcDNA3-OGR1 (human) and pcDNA3-GPR4 (human) plasmids were generated in our laboratory as described previously (12,21–23). OGR1-pMSCV murine stem cell virus retroviral vector (MSCV; puromycin) expression plasmids with or without fusion to enhanced green fluorescence protein (EGFP) were constructed. To construct the pMSCV-3HA-OGR1-EGFP plasmid, the 3HA-OGR1-EGFP fragment of the pEGFP-N1-3HA-OGR1 plasmid, which we constructed previously (our unpublished results), was removed by digestion with *Not*I and *Xho*I and was then inserted into the pTriEx-1 vector (Novagen, San Diego, CA). Similarly, to construct the pMSCV-3HA-OGR1 plasmid, the 3HA-OGR1 fragment was removed from pcDNA3-OGR1 by digestion with *Hind*III and *Eco*RI and was then inserted into the pTriEx-1 vector. Both the 3HA-OGR1 and the 3HA-OGR1-EGFP DNA fragments were then excised from the pTriEx-1 vector and inserted into pMSCV (puromycin) by digestion with *Eco*RI and *Xho*I. The EGFP-coding sequence fragment was amplified from the pEGFPN1 plasmid (BD Biosciences, Palo Alto, CA, GenBank accession code U55762) by polymerase chain reaction (PCR) using primers 5′-ACAGTTTAA ACTTCGAATTCTGCAGTCGACGG-3′(forward) and 5′-AAT GCGGCCGCTTTACTTGTACAGCTCGTCCATGC-3′ (reverse) and then cloned into pMSCV (puromycin) by *Eco*RI and *Xho*I digestion. The resulting plasmid pMSCV-EGFP was used as the EGFP control vector. An OGR1 mutant, pcDNA3-OGR1-H245F was constructed by site-directed mutagenesis. The histidine residue of OGR1 at position 245 was replaced with phenylalanine using the Quick Change Mutagenesis System (StrataGene Systems Inc, La Jolla, CA) and the pcDNA3-OGR1 plasmid as the template. The mutagenesis was confirmed by sequence analysis.

All plasmid constructs were transformed in DH5α (Invitrogen, Carlsbad, CA)-competent *Escherichia coli*, and selected colonies were cultured. Plasmid DNA was purified using either the GenElute Five-Minute Plasmid Miniprep Kit (Sigma) or QIA prep MINIprep (Qiagen, Valencia, CA). The DNA sequences and reading frames were verified by sequence analysis at the Molecular Biotechnology core facility at the Cleveland Clinic using an ABI Prism 377 Automated DNA Sequencer (Applied Biosystems, Foster City, CA).

Transient Transfection and Generation of Stable Clones

HEK293T cells were cotransfected with each of the plasmid constructs pMSCV-3HA-OGR1, pMSCV-3HA-OGR1-EGFP, pMCV-EGFP, or pMSCV empty vector and packaging plasmid using a calcium phosphate transfection kit (Invitrogen) according to the manufacturer's instructions. The media containing the virus were collected 3 days after transfection, and the viral particles were collected by centrifugation at 1620*g* for 30 minutes at 4 °C. PC3 cells were plated into six-well tissue culture dishes and infected with 1–2 mL of the virus-containing media from transfected HEK293 cells. Infected cells were transferred to 10-cm dishes 3 days later. Stable single PC3 cell colonies (monoclonal) or pooled cells (polyclonal) were selected with puromycin (2.5 μg/mL). Clones expressing OGR1 or vector were designated as OGR1-PC3, OGR1-EGFP-PC3, vector-PC3, and EGFP-PC3. For PC3 cell–transient transfection, PC3 cells were transfected with 1.0–1.5 μg of pcDNA3-OGR1, pcDNA3-GPR4, or pcDNA3-OGR1-H245F or were cotransfected with pcDNA3-OGR1 and pcDNA3-$G\alpha_{i1}$ dominant-negative plasmids in six-well plates using lipofectamine 2000 (Invitrogen) according to the manufacturer's protocol. C4-2 and DU145 cells were transiently transfected with 1.0–1.5 μg of the pcDNA3 empty vector or the pcDNA3-OGR1 plasmid. Cellular assays were conducted 48–72 hours after transfection.

Human Prostate Cancer Metastasis Orthotopic Mouse Model

All mouse studies were approved by the Indiana University School of Medicine or the Cleveland Clinic Institutional Animal Care and Use Committees. In these studies, 5- to 7-week-old male athymic (nu/nu, n = 26) or NOD/SCID (n = 32) mice were anesthetized using isoflurane (2%–4%), nembutal (50 mg/kg), or ketamine (200 mg/kg). An abdominal incision (5–10 mm) was made in each mouse, and the prostate gland was exposed and injected once with either OGR1-PC3 (n = 7), OGR1-EGFP-PC3 (n = 25), vector-PC3 (n = 3), or EGFP-PC3 (n = 23) cells (5.0×10^6 cells in 40–50 μL phosphate-buffered saline [PBS: sodium chloride, 145 mM {0.85%} in phosphate buffer, 150 mM {Sigma}]). After injection, prostate glands were placed back into the peritoneal cavity, and the incisions were surgically closed.

Postsurgical and Necropsy Procedures

Following tumor cell injection, mice were observed daily for signs of tumor development, including hunched posture, abdominal bloating, or loss of mobility. Mice were killed on day 45 when tumors had metastasized to other organs in the control mice by CO_2 inhalation, and necropsies were performed to assess tumor growth and metastasis. Metastases in different organs were measured and counted using fluorescence or light microscopy. All primary prostate tumors and metastases were harvested, fixed in 10% neutral buffered formalin, embedded in paraffin, sectioned into 5-μm slices, and then either stained with hematoxylin and eosin or immunostained using antibodies as described below. Bones (ribs, tibia, and femur) from mice injected with control EGFP-PC3 or OGR1-EGFP-PC3 clones were removed, dissected free of most adherent tissues, and observed immediately with epifluorescence microscopy. In addition, bones were fixed in 4% paraformadehyde and decalcified in 14% EDTA (pH 7.4) for 2 weeks at 4 °C. The decalcified bones were sectioned and observed using epifluorescence microscopy.

Microscopy and Reverse Transcription–Polymerase Chain Reaction to Detect Metastases

Tumors expressing EGFP were observed using a Leica fluorescent stereomicroscope equipped with green (fluorescein, 480Ex/530Em)

and red (TexasRed, 560Ex/630Em) filters (model MZ 16FA). The green and red images were merged, and the metastases in the mice that had been injected with OGR1-EGFP-PC3 and EGFP-PC3 were compared using Image ProPlus software (Media cybernetics, Bethesda, MD). A light stereo microscope (model SMZ1000, Nikon, Fryer Co Inc, Huntley, IL) equipped with a Nikon digital camera (DXM1200F) was used to analyze tumor size and metastases to different organs. For quantification of in vitro fluorescence, images were captured from four fields per well (three wells per sample) at ×40 magnification using a Nikon epifluorescence microscope. Images were saved in JPEG format and converted into Canvas 9 (ACD System, Miami, FL) format for analysis. Background fluorescence was approximated from a well of control PC3 cells (i.e., that had not been transfected with an EGFP-containing vector) and subtracted from the levels of fluorescence from test cells.

To detect potential microscopic tumors, small portions of liver (three to four portions per mouse) were collected from seven to eight mice from each group of EGFP-PC3 or OGR1-EGFP-PC3. Total RNA was isolated, and reverse transcription (RT)–PCR was carried out using primers specific for EGFP and β-actin. The primers for EGFP were 5′-CCT ACG GCG TGC AGT GCT TCA GC-3′ (forward) and 5′-CGG CGA GCT GCA CGC TGC GTC CTC-3′ (reverse). The primers for β-actin were 5′-AAG GCC AAC CGT GAA AAG ATG ACC-3′ (forward) and 5′-ACC GCT CGT TGC CAT TAG TGA TGA-3′ (reverse) (GenBank accession number NM_007393).

In Vivo Primary Tumor Cell Proliferation Assay

Cell proliferation in primary prostate tumors was assessed using 5-bromo-2-deoxyuridine (BrdU; Sigma) staining. Mice were injected intraperitoneally with 40 mg/kg body weight of BrdU. After 2 hours, mice were killed as described above, and primary prostate tumors were excised, formalin fixed, and embedded in paraffin (from each primary tumor of seven to eight mice per group).

Immunohistochemistry for OGR1, 5-Bromo-2-Deoxyuridine, and Natural Killer Cells

Immunostaining was performed on primary tumor sections using the Vectastain Universal ABC kit (Vector Laboratories). Briefly, paraffin-embedded tissues were deparaffinized with xylene or Histo-Clear (National Diagnostics, Atlanta, GA) and dehydrated using decreasing gradient alcohol washes (100%, 95%, and 80% ethanol). Antigen retrieval was performed by microwaving the sections in 10 mM citrate buffer for 1 minute. Sections were then blocked with horse serum (included in the Vectastain Universal ABC kit) (2.5% in PBS) and incubated overnight with rabbit anti-human OGR1 polyconal antibody (1:500 dilution) or for 30 minutes with rat anti-mouse monoclonal CD49b (NK1.1, 1:250 dilution) or mouse monoclonal anti-BrdU sera (1:500). Sections were then incubated with biotinylated pan-specific universal secondary antibody (according to the user manual from Vector Laboratories) for 10 minutes, followed by incubation with streptavidin–peroxidase for 5 minutes and 3, 3′-diaminobenzidine. The staining levels in the negative controls (duplicate slides without primary antibodies) were used as background. All cells that stained brown were considered positive. Immunostaining was scored (×20 magnification) on triplicate tissue sections from each group of mice by an independent observer blindly (Dr Weiling Xu).

Terminal Transferase dUTP Nick End Labeling Assay to Detect Cells Undergoing Apoptosis

Terminal transferase dUTP nick end labeling assays were performed to detect apoptotic cells in the primary tumors by using an Apoptag Peroxidase In Situ Apoptosis Detection Kit (Chemicon, Temecula, CA). Tumor sections (from seven to eight mice per group) were deparaffinzied and rehydrated as mentioned above and then incubated in 20 μg/mL proteinase K for 15 minutes at room temperature and washed twice with distilled water. Next, the endogenous peroxidase activity in the tumor sections was blocked by incubation for 5 minutes with 3% H_2O_2 in PBS, followed by incubation for 10 seconds with equilibration buffer. The sections were then incubated for 1 hour at 37 °C with terminal deoxynucleotidyl transferase enzyme in reaction buffer (according to the manufacturer's instructions). The reaction was terminated by incubation with stop buffer at room temperature. Sections were then incubated with peroxidase-conjugated anti-digoxigenin antibody for 30 minutes, and the reaction was developed with diaminobenzidine substrate for 4 minutes at room temperature.

RNA Isolation and RT–PCR to Measure OGR1 and EGFP mRNA Expression

Total RNA was extracted from 5.0×10^5 to 6.0×10^5 OGR1-PC3, vector-PC3, DU145, and C4-2 cells or from 2.5 mg of primary tumors or livers from mice injected with vector-PC3 and OGR1-PC3 clones using the total SV RNA isolation kit (Promega, Madison, WI) following the manufacturer's protocol. First-strand cDNA was synthesized from 2.5 μg DNA-free total RNA using the SuperScript II first-stand synthesis kit (Invitrogen). OGR1 expression levels were analyzed by semi-quantitative RT–PCR. Glyceraldehyde-3-phosphate dehydrogenase served as the loading control. RT–PCR for the OGR1-EGFP fusion protein was performed with an OGR1-specific forward primer (5′-TCCGGGAAAAGCGGGGC-3′) and an EGFP-specific reverse primer (5′-TGCAGAAATTCTTACTTGTACAGCTCGTCCA TG-3′). For OGR1, RT–PCR was performed using OGR1-specific forward (5′-CTGCCTGTCCCTCTACTTCG-3′) and reverse (5′-TGTTCTCGTACAGGAGGATGC-3′) primers. Quantitative PCR was performed with primers obtained from Gorilla Genomics, Inc (Alameda, CA). The primer sequences for OGR1 were 5′-CACCGTGGTCATCTTCCTG-3′ (forward) and 5′-GGAGAAGTGGTAGGCGTTGA-3′ (reverse). The β_2-microglobulin housekeeping gene (NM_004048) was used as the loading control. The primer sequences used to amplify the β_2-microglobulin were 5′-ACTGGTCTTTCTATCTCTTGTACT-3′ (forward) and 5′-CTGCTTACATGTCTCGATCC-3′ (reverse). Experiments were performed three times in triplicate for each cell line. The primers used for measuring EGFP mRNA in the liver tissues were 5′-GACGACGGCAACTACAAGA-3′ (forward) and 5′-GATGCCGTTCTTCTGCTT-3′ (reverse). PCR was performed with RNA isolated from three to four portions of each liver per mouse from 16 mice per group.

Immunoblot for G protein alpha–inhibitory subunit 1

Vector-PC3 and OGR1-PC3 cells (at 80%–85% confluence in a six-well plate) were treated with or without actinomycin D (500 ng/mL Calbiochem, San Diego, CA) for 24 hours. Total protein was extracted and quantified using the BCA Protein Assay Kit (Pierce, Rockford, IL). Equal amounts of protein per lane were separated on 10% sodium dodecylsulfate minigels and then electrophoretically transferred to Immobilon P polyvinylidene difluoride membranes (Millipore, Billerica, MA). Membranes were blocked in 5% nonfat dry milk in Tris-buffered saline containing 0.2% Tween 20 (TBST) for 2 hours at room temperature and then incubated with rabbit polyclonal anti-$G\alpha_{i1}$ antibody overnight at 4 °C (1:1000 dilution), washed three times with TBST, incubated with goat anti-rabbit IgG horseradish peroxidase–conjugated secondary antibody (1:4000 dilution), and finally washed three times with TBST. Antibody–protein complexes were visualized using the ECL Western Blotting Detection System (Amersham Biosciences, Piscataway, NJ). The membranes were then stripped and reblotted with monoclonal mouse β-actin antibody (1:3000 dilution) to assess protein loading and transfer. Immunoblotting was performed three times using vector-PC3, EGFP-PC3, OGR1-PC, and OGR1-EGFP-PCs cells.

pH Effect Studies

To test the effect of pH on the secretion of arachidonic acid (AA) and LPC in OGR1-PC3 cells, physiologic salt solutions (PSS; 130 mM NaCl, 0.9 mM NaH_2PO_4, 5.4 mM KCl, 0.8 mM $MgSO_4$, 1 mM $CaCl_2$, 25 mM glucose, and 20 mM HEPES) at three different pHs (6.8, 7.4, and 7.8) were prepared (25). Vector-PC3 and OGR1-PC3 cells were incubated with each of the PSS for 90 minutes in a humidified 5% CO_2 atmosphere chamber at 37 °C. Cell supernatants were collected, and AA and LPC were extracted as described below. Five independent experiments were performed in triplicate.

Preparation of Conditioned Media

Vector-PC3 and OGR1-PC3 cells were grown in 10-cm^2 tissue culture plates to 85%–95% confluence. The media was then removed, the cells were washed twice with PBS, and serum-free RPMI-1640 medium containing 100 units/mL penicillin–streptomycin and 2 mM glutamine (6 mL) was added to each plate. The conditioned medium was collected after 12–16 hours of incubation and stored at –80 °C in glass or siliconized plastic tubes before analysis. For experiments using pertussis toxin (PTX) treatment, vector-PC3 and/or OGR1-PC3 cells were plated as above and pretreated with 100 nM PTX for 16 hours. The PTX media was removed, and the cells were washed twice with PBS and incubated in either serum-free or complete medium (RPMI-1640 with 10% FBS), and medium was collected as described above. This procedure was performed three times in triplicate.

Migration Assay

Parental PC3 cells and PC3 clones were cultured to 85%–95% confluence and subjected to serum starvation for 16 hours before assay. Cells were dissociated by incubation with trypsin–EDTA (0.05% trypsin, 53 mM EDTA), washed twice with PBS, and counted using a hemocytometer. The lower side of the insert of the 24-well transwell migration chamber membrane (8.0 μm pore size; Corning Inc, New York, NY) was coated with 10 μL of 10 μg/mL vitronectin (Chemicon,) and dried at room temperature. Vitronectin was chosen among several ECM proteins tested because it was the substrate on which OGR1 had the maximal inhibitory effect on cell migration; thus, differences between groups could be readily observed. Serum-free media (300 μL) was added to each lower chamber of the 24-well transwell. Inserts (the upper chambers) were then placed in the wells (the lower chambers). Cells (0.5×10^5 to 1.0×10^5 in 300 μL serum-free media) were added to each upper chamber and incubated for 4.5 hours. Nonmigrating cells were removed with a cotton swab. The cells that migrated to the lower phase of the upper chamber were then fixed in methanol for 30 minutes and stained with crystal violet (1 g/mL, Fluka Chemical Corp, Milwaukee, WI) for 30 minutes at room temperature. Excess stain was removed with water, and the chambers were air-dried. Cells were then visualized under the microscope and quantified by counting the number of cells in three randomly chosen fields. At least 10 independent experiments were performed, each in triplicate.

To study the effect of conditioned media on cell migration, parental PC3 cells were serum starved for 16 hours, treated with trypsin–EDTA, washed twice with PBS, counted, and then preincubated with conditioned media (see above) or lipid extracts from conditioned media (see below for lipid extraction) for 30 minutes on a rotator in a cell culture incubator before being used for migration assays. At least eight independent experiments were performed, each in triplicate.

Transendothelial Migration Assay

A monolayer of HMEC-1 cells was generated on 24-well transwell migration chambers by seeding 5.0×10^6 cells. Control EGFP-PC3 or OGR1-EGFP-PC3 cells were added directly on top of the endothelial cell layer, as described above. Non-GFP cells were treated with calcein AM (10 μmol/mL) (Invitrogen) for 30 minutes, washed twice, and then added on top of the endothelial cell layer. Migrated cells were fixed with methanol for 20 minutes and counted using a fluorescence microscope. Three independent experiments were performed, each in triplicate.

In Vitro Cell Proliferation Assay

OGR1-PC3, OGR1-EGFP-PC3, vector-PC3, and EGFP-PC3 clones were seeded in 48-well plates (5000 cells per well). After 6 hours, the medium was replaced with RPMI-1640 supplemented with or without 2% FBS. Cells were stained with 2% trypan blue and cell proliferation at 24, 48, and 72 hours was assessed by counting using a hemocytometer or by MTT assay. For the MTT assay, 30 μL of MTT (5 mg/mL in PBS) was added to each well containing 200 μL media and incubated at 37 °C for 3 hours. After the cell culture medium was removed, 200 μL of dimethyl sulfoxide was added to each well to solubilize the dye. Absorbance was examined at 570 nm using a Victor3 plate reader (PerkinElmer Life and Analytical Sciences, Shelton, CT). Three independent experiments were performed (using EGFP-PC3 and OGR1-EGFP-PC3 cell lines) in triplicate.

Heat Treatment, Lipid Extraction From Conditioned Media, and Mass Spectrometry Analyses

To study the effect of heat-treated conditioned media on parental PC3 cell migration, conditioned media from OGR1-PC3,

OGR1-EGFP-PC3, vector-PC3, or EGFP-PC3 cells were heated in an immersion circulating water bath (PolyScience, Niles, IL) at 95 °C for 30 minutes. The media were centrifuged at 13 400*g* for 10 minutes at 4 °C and used for migration assays. At least five independent experiments were performed for each cell line, each in triplicate.

LPC was extracted from the conditioned media from vector-PC3 or EGFP-PC3 and OGR1-PC3 or OGR1-EGFP-PC3 using the method of Bligh and Dyer (26). In brief, 10 μL of 12 : 0 LPC (1 μM) was added (as an internal standard, IS) to 1.8 mL conditioned medium, which was mixed with 3 mL of methanol/chloroform (2 : 1). The samples were mixed by vortexing for 1 minute and incubated on ice for 10 minutes. Chloroform (1 mL) was added to separate the phases, and the samples were mixed by vortexing for 1 minute and then centrifuged (1750*g* for 10 minutes, at 4 °C). The lower phase was transferred to a new glass tube. The upper phase was re-extracted and the lower phases were combined. The experiment was performed at least seven times independently, each in triplicate. Arachidonic acid was extracted using ethyl acetate (27). In brief, 1 mL of conditioned medium from each sample was mixed with 3 mL of ethyl acetate, and 10 μL of HCl was added. The samples were vortexed for 1 minute and then centrifuged (1750*g* for 10 minutes, at 4 °C). The upper phase was transferred to a new glass tube, the solvent was evaporated under nitrogen at room temperature, and the dried lipids were resuspended in 100 μL of methanol for mass spectrometry (MS) analyses.

MS analyses of lipid extracts from conditioned media samples were performed using API-4000 LC-MS–MS (Applied Biosystems/MDS SCIEX). Data processing was highly automated using the mass spectrometer software and Excel. Samples (10 μL) were directly delivered into the electrospray ionization source through the LC system (Agilent 1100) with an autosampler. The mobile phase was methanol/water/AmOH (90 : 10 : 0.1, vol/vol/vol) with a flow rate of 0.1 mL/min and 3 minutes for each sample. Quantitative analyses were performed using the methods described previously (28,29) in the multiple reaction monitoring mode. The peak intensity ratios (standard/IS) versus the concentration ratios (standard/IS) were plotted and fitted using linear regression. At least seven independent experiments were performed, each in triplicate.

Statistical Analysis

Data are presented as means with 95% confidence intervals (CIs) of at least three independent experiments. Different values among groups were compared using Student's *t* test. All statistical tests were two-sided, and *P* values less than .05 were considered to be statistically significant.

Results

The Metastatis Suppressive Role of OGR1 In Vivo

Expression of OGR1 has been shown to be fivefold lower in metastatic tumors than in primary prostate tumors (24), implying that OGR1 may have an inhibitory role in tumor metastasis. To investigate the direct role of OGR1 in tumor metastasis, we established several PC3 cell clones that stably overexpress OGR1. PC3 cells were chosen because of their high metastatic potential and because they have been used successfully in mouse models of metastatic prostate cancer (30). All the OGR1-PC3 clones used in this report expressed 4-fold to 10-fold more OGR1 mRNA than parental PC3 cells, as assessed by quantitative PCR (data not shown).

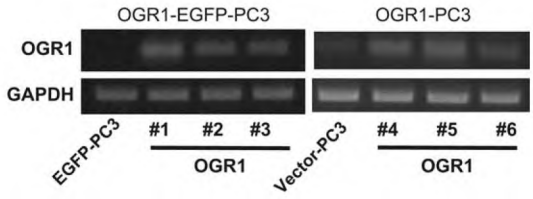

Fig. 1. Ovarian cancer G protein–coupled receptor 1 (OGR1) mRNA expression in PC3 clones. PC3 human prostate cancer cells were transfected with one of the following DNA constructs: control retrovirus vector–enhanced green fluorescence protein (pMSCV-EGFP), pMSCV alone, pMSCV-OGR1-EGFP, or pMSCV-OGR1. Stable clones were selected by puromycin treatment (2.5 μg/mL). OGR1 expression in stable clones was analyzed by reverse transcription–polymerase chain reaction. Controls were clones selected from PC3 cells transfected with control vectors pMSCV and pMSCV-EGFP. Samples #1 and #2 were single stable clones and sample #3 was pooled (mixing several different single stable EGFP-positive) OGR1-EGFP-PC3 clones. Samples #4, #5, and #6 were OGR1-PC3 clones (without EGFP). The housekeeping gene glyceraldehyde-3-phosphate dehydrogenase (GAPDH) was used as the loading control. One representative image of three independent experiments is shown.

Stable clones of PC3 cells that were transfected with vector controls (vector-PC3 and EGFP-PC3) expressed very low levels of endogenous OGR1 mRNA (Figs. 1 and 2, G). However, cells that were transfected with OGR1 expression vectors (OGR1-PC3 or OGR1-EGFP-PC3) overexpressed OGR1 (Fig. 1). To avoid differential effects resulting from different OGR1 insertion sites across clones, both selected single-cell clones and a pooled clone (a pool of several selected single-cell clones) of PC3 cells were used in subsequent experiments. OGR1 was fused to EGFP to enable easy observation and analysis of PC3-derived primary and metastatic tumors using fluorescence microscopy. However, to avoid potential EGFP-related nonspecific effects, we also transfected cells with OGR1 plasmids without the EGFP fusion (OGR1-PC3 clone).

To study the effect of OGR1 on tumoriginesis and metastasis in vivo, we used mouse models of metastatic prostate cancer. Athymic and NOD/SCID mice were randomly divided into two groups (three to eight mice per group), and PC3 clones were injected orthotopically into the prostate gland of each mouse. Forty-five days later, mice were killed and tumor development was examined. Mice that had been injected with vector-PC3 or EGFP-PC3 formed primary tumors in the prostate glands and metastatic tumors in the liver, spleen, kidney, stomach, lung, lymph nodes, diaphragm, and mesentery (Fig. 2, A–C; arrows indicate tumor loci). In contrast, the mice that were injected with the OGR1-PC3 or OGR1-EGFP-PC3 clones developed tumors that were confined to the prostate gland and did not metastasize to any of the other organs examined (Fig. 2, A–C). To rule out a potential nonspecific effect of EGFP, we also tested the effect of OGR1-PC3 (without EGFP fusion) cells in mice, using the vector-PC3 cells as the control.

We conducted four independent sets of experiments (Table 1) in athymic and NOD/SCID mice. Overall, we observed a statistically significant reduction in metastases when exogenous

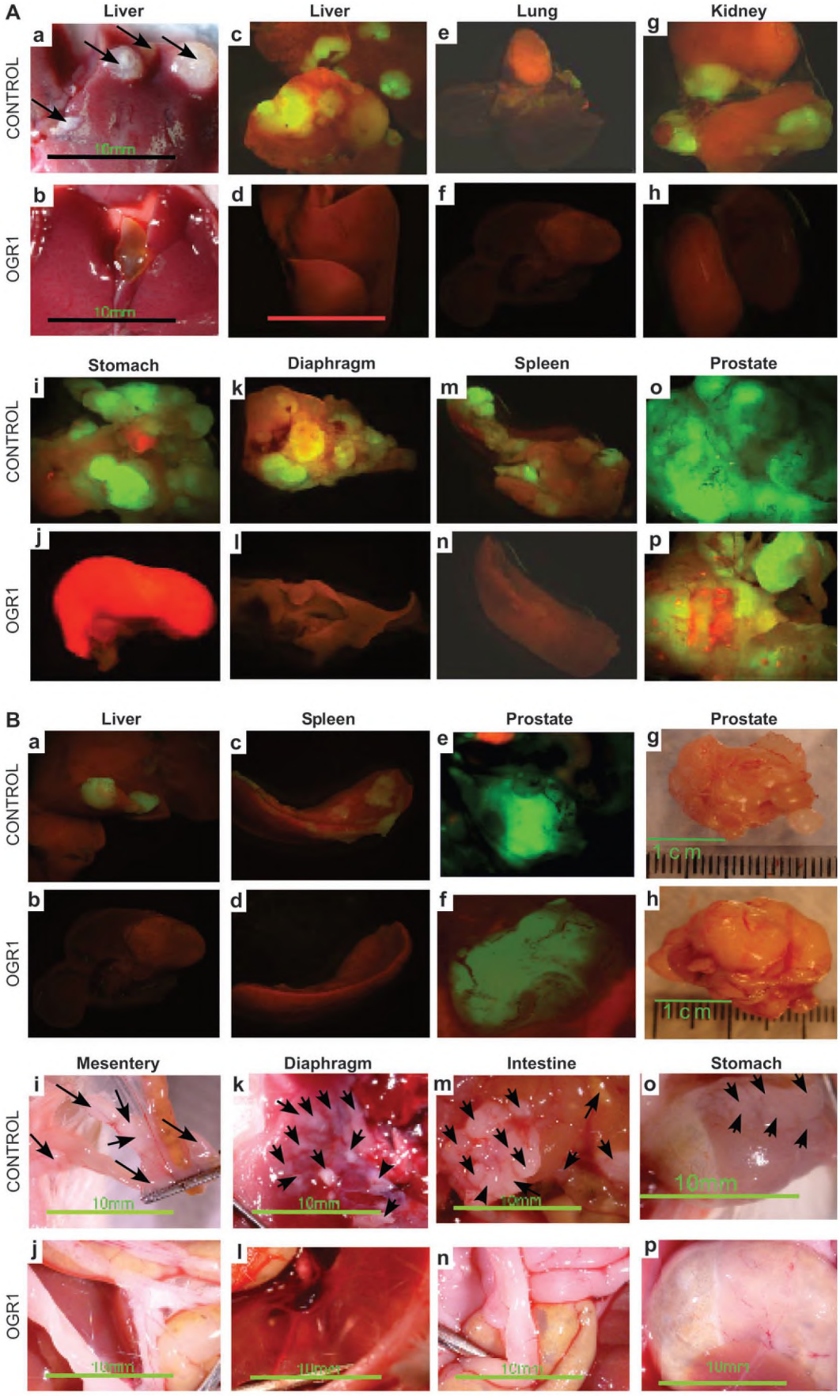

Fig. 2 (continues)

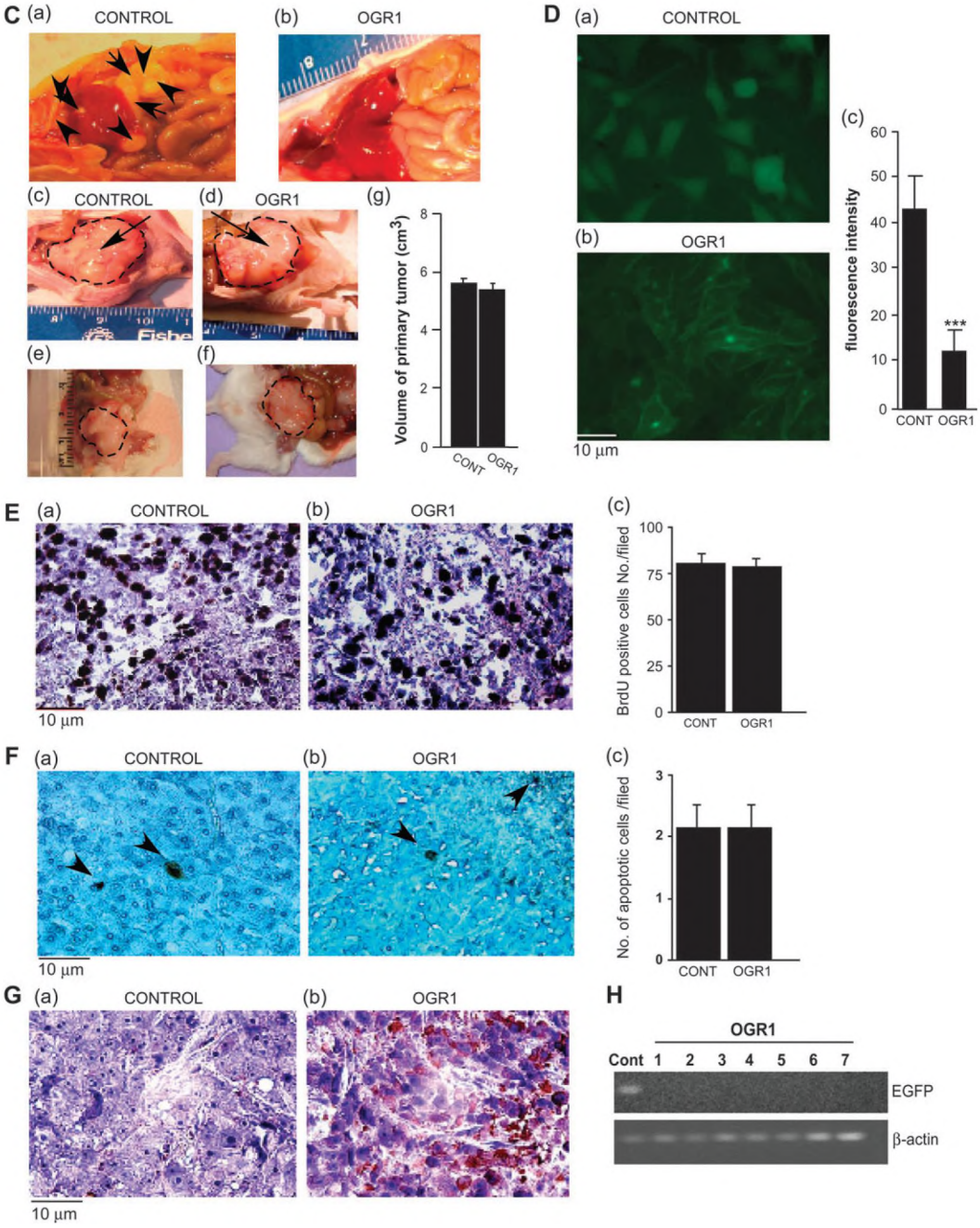

Fig. 2. Ovarian cancer G protein–coupled receptor 1 (OGR1) expression and PC3 cell metastasis in vivo. PC3 cells (5.0×10^6) from clones expressing enhanced green fluorescence protein (EGFP) as a control (CONTROL) or clones expressing OGR1-EGFP (OGR1) were injected into the prostate lobes of 5- to 8 week-old athymic or NOD/SCID mice. **A** and **B**) On day 45 after injection, athymic mice (**A**) or SCID mice (**B**) were analyzed for metastasis to different organs or anatomic regions. Examination of tumor development in different organs was performed by light stereo microscopy (**A, a** and **b** and **B, i–p**) or fluorescence stereo microscopy (**A, c–p** and **B, a–f**). **C**) Images of metastatic tumors (**a** and **b**) and primary prostate tumors (athymic mice, **c** and **b**; NOD/SCID mice, **e** and **f**) are shown. **Arrows** indicate the tumors derived from PC3 cells implanted into the prostate. The area surrounded by the **dotted lines** indicates the primary prostate tumor. The size of the primary tumor was quantified, and mean (95% confidence intervals) volumes are shown in (**g**). **D**) EGFP expression in stable clones of control EGFP-PC3 and OGR1-EGFP-PC3 in vitro. Equal number of cells were seeded in a six-well plate, and images of the cells were captured with an epi-fluorescence microscope using ×40 magnification (**a** and **b**). Mean (and 95% confidence intervals) fluorescence intensity is shown (**c**). **E**) In vivo primary prostate tumor cell proliferation assays were carried out by injecting BrdU (intraperitoneally, 40 mg/kg body weight), which is incorporated by proliferating cells (**a** and **b**). BrdU-positive cells were quantified, and the mean (and 95% confidence interval) number of stained cells is shown (**c**). **F**) Terminal transferase dUTP nick end labeling assay of the primary tumor sections was performed to detect apoptotic cells. The brown color stained cells indicate the cells undergoing apoptosis (**arrow head**). Mean (and 95% confidence intervals) numbers of apoptotic cells per field are shown (**c**). **G**) OGR1 protein expression in prostate tumors from mice injected with control (either vector-PC3 or EGFP-PC3) or OGR1-PC3 (either OGR1-PC3 or OGR1-EGFP-PC3) cells were analyzed by immunohistochemistry with an anti-human OGR1 antibody. **H**) Detection of potential miscroscopic metastatic tumors. Small portions of the livers without overt tumors from mice injected with control and OGR1-PC3 cells were collected, and total RNA was isolated. A liver metastatic tumor from a control mouse was used as a positive control (Cont). Reverse transcription–polymerase chain reaction was conducted using specific primers for EGFP and β-actin. Samples in **lanes 1–7** are from tissues without overt tumors. Five independent experiments were performed.

OGR1 was expressed in PC3 cells as compared with control cells. Metastatic foci were not found in any organ (other than the prostate) in 28 out of 32 mice in OGR1 groups (OGR1-EGFP-PC3 and OGR1-PC3 as single-cell clones or a pooled clone) (Table 1). The remaining four mice in this group developed several small tumors (mean = 12.50%, 95% CI = 4.08% to 29.93%) that were localized to the mesentery (≤2mm in size) (Table 1). In contrast, all 26 control mice (mean = 100%, 95% CI = 83.97% to 100%) injected with vector- or EGFP-PC3 cells had numerous metastatic foci in multiple organs (Table 1). In addition, the metastases in control mice were larger (≥2 mm) and often fused together to form tumor aggregates (Fig. 2, A and Table 1). We did not observe bone metastases in either the control or the OGR1 mice (data not shown), which is consistent with previous reports using the same PC3 injection model (31,32). In addition, we tested the potential existence of microscopic tumors using PCR-based detection of EGFP in the liver samples collected from both control (EGFP-PC3) and OGR1 (OGR1-EGFP-PC3) groups. Although EGFP was detected in overt tumors, no EGFP was detected in liver samples that appeared to be tumor free, suggesting the absence of microscopic tumors (Fig. 2, H).

We obtained similar results in athymic mice and NOD/SCID mice (Fig. 2, B and Table 1), which do not have normal T and B cells, suggesting that both T and B cells do not play an important role in OGR1's metastatis suppression effect. In addition, we performed immunohistochemistry using the CD49b (NK1.1) antibody and found no difference in the number of natural killer (NK) cells in tumor sections derived from control cells and OGR1-expressing cells (data not shown), suggesting that NK cells may also do not play an important role in OGR1's metastasis suppression effect.

We next compared growth of primary tumors in mice that were injected with either vector control or OGR1-PC3 cells. These mice developed primary prostate tumors that were similar in size, suggesting that OGR1 did not affect primary tumor growth (Fig. 2, A, o and p; Fig. 2, B, e–h; Fig. 2, C, c–f; Table 1). The fluorescence intensity of the primary tumors in the OGR1 mice appeared lower than that of the control mice (compare Fig. 2, A, o and p and Fig. 2, B, e and f). This difference was mainly due to lower EGFP expression in the OGR1-EGFP-PC3 cells compared with that in EGFP-PC3 cells (Fig. 2, B and D).

To further evaluate the effect of OGR1 overexpression on primary tumor cell proliferation, we conducted BrdU incorporation and terminal transferase dUTP nick-end labeling assays in xenograft tumors from the athymic or the NOD/SCID mice. We observed that primary prostate tumors derived from vector control and OGR1-PC3 cells had similar BrdU incorporation (Fig. 2, E). Minimal apoptosis was detected in tumor sections derived from both control and OGR1-expressing cells (Fig. 2, F), confirming that OGR1 did not affect growth and apoptosis of the primary tumors.

Thus, by the definition of metastasis suppressor gene (3,7), our data support the hypothesis that OGR1 is a novel metastasis suppressor gene in prostate cancer. We also confirmed that tumors derived from OGR1-PC3 cells still expressed OGR1 as assessed by immunohistochemical staining (Fig. 2, G).

Table 1. Summary of analysis for metastasis and primary tumor size in prostate cancer orthotopic mouse model using athymic and SCID mice*

Characteristic	Control (N = 26)	OGR1 (N = 32)	P†
Mice with metastases			
Number	26 of 26	4 of 32	<.001
Percent (95% CI)	100 (83.97 to 100)	12.50 (4.08 to 29.9)	
Percent reduction		87.5	
Metastases per mouse			
≤2 mm, mean (95% CI)	101.4 (91.8 to 111.0)	.56 (0.40 to 0.72)	<.001
>2 mm, mean (95% CI)	114.5 (107.9 to 121.0)	0 (0.0 to 0.0)	<.001
Primary tumor size, cm^3			
Mean (95% CI)	5.25 (5.07 to 5.42)	5.20 (4.99 to 5.41)	

* Metastases were found in the liver, mesentery, intestine, stomach, spleen, lymph node, kidney, diaphragm, and lung. In the control group, 16 SCID and seven athymic mice were injected with EGFP-PC3 cells; three athymic mice were injected vector-PC3 cells. In the OGR1 group, 16 SCID and five athymic mice were injected with single clones of OGR1-EGFP-PC3 cells, four athymic mice were injected with pooled clones of OGR1-EGFP-PC3 cells, and seven athymic mice were injected with OGR1-PC3 cells. SCID = severe combined immunodeficiency; OGR1 = ovarian cancer G protein–coupled receptor 1; CI = confidence interval; EGFP = enhanced green fluorescence protein.

† *P* values (two-sided) were calculated using Student's *t* test.

The Effect of OGR1 on Cell Migration and the Involvement of $G\alpha_i$ Protein in the Inhibitory Effect

To determine the molecular mechanisms by which OGR1 suppresses tumor metastasis, we examined the effect of OGR1 on cell migration in vitro. We tested PC3 cell migration to several extracellular matrix (ECM) proteins (fibronectin, laminin, vitronectin, collagen I, and collagen IV) using transwell assays. OGR1 expression, either with or without fusion to EGFP, statistically significantly inhibited cell migration to vitronectin reduction compared with the controls (mean percentage of cells migrated, 30.2% versus 100%, difference = 69.8%, 95% CI = 63.0% to 75.9%; $P<.001$; Fig. 3, A and C (CONT; data from both vector-PC3 and EGFP-PC3 were taken as 100%. OGR1#1 = OGR1-PC3 and OGR1#2 = EGFP-OGR1-PC3). Other ECM proteins either induced low levels of haptotaxis of the parental cells, and OGR1 expression did not induce as much of an effect with the other ECM proteins as it did with vitronectin (data not shown). Thus, vitronectin was chosen as the ECM for the remainder of the migration assays. In contrast to OGR1, expression of GPR4, the G protein–coupled receptor sharing the highest homology with OGR1, did not affect PC3 cell migration to vitronectin, suggesting a specific function of OGR1 (Fig. 3, A and B). We also conducted transendothelial migration assays to mimic the intravasation process in vivo and found that OGR1 also inhibited this activity to a similar extent (70% inhibition) (Fig. 3, C). In addition, we performed cell migration assays with C4-2 and DU145 prostate cancer cell lines (which do not express endogenous OGR1, as assessed by PCR; data not shown) and found that OGR1 statistically significantly inhibited migration in both cell types similar to that of PC3 cells (70% reduction in migration, $P<.001$ for both C2-4 and DU145) (Fig. 4, A),

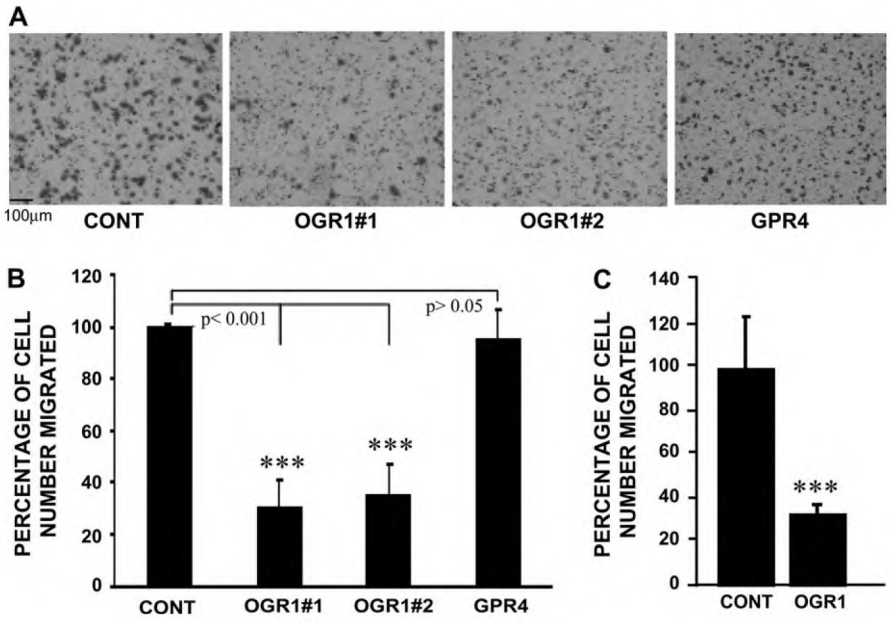

Fig. 3. The effect of ovarian cancer G protein–coupled receptor 1 (OGR1) in cell migration to vitronectin and the involvement of G protein alpha–inhibitory subunit 1. Migratory properties of vector- and OGR1-PC3 cells to vitronection were assessed using transwell assays. Stably transfected vector control-PC3 or OGR1-PC3 cells were serum starved for 16 hours. Cells (1×10^5) in 300 μL of serum-free RPMI were added to the upper chamber of a vitronectin-coated transwell, and 300 μL of serum-free RPMI was added in the lower chamber. **A**) Cell migration of control (CONT, vector-PC3 or EGFP-PC3) and two stable clones of OGR1-PC3 cells (OGR1#1; OGR1-PC3, and OGR1#2; OGR1-EGFP-PC3) and GPR4-PC3 (GPR4) are shown. To compare effects of OGR1 and GPR4, cells were transiently transfected with OGR1 and GPR4 expression vectors or empty pcDNA3 vector as control and serum starved, and migration assays were conducted 48 hours after transfection. **B** and **C**) Cell migration [transwell (**B**) and transendothelial (**C**)] in OGR1-PC3 cells compared with parental or vector-PC3 cells (***P<.001). P values were calculated using two-sided Student's t test). More than 10 independent experiments were performed in triplicate.

suggesting that OGR1's inhibitory effect on cell migration is not limited to PC3 cells.

To explore the mechanism of this inhibition, we tested the effect of PTX on the cell migration of vector- and OGR1-PC3 cells. PTX pretreatment stimulated cell migration of OGR1-PC3 cells but had no effect on vector-PC3 cells, suggesting that activating $G\alpha_i$ proteins, which are sensitive to PTX, are involved in OGR1-induced inhibition of cell migration. To confirm this result, cells were transfected with a dominant-negative form of $G\alpha_{i1}$ and cell migration was monitored as before. The dominant-negative form of $G\alpha_{i1}$ reversed the effect of OGR1 (Fig. 4, B), similar to that seen with PTX, confirming the involvement of a $G\alpha_{i1}$ protein in OGR1's inhibitory effect. Because migration is a critical step in tumor metastasis, the reduced cell migration in vitro may be related to the reduced tumor metastasis that was observed in vivo. To explore how OGR1 regulates $G\alpha_{i1}$, we tested whether OGR1 expression alters $G\alpha_{i1}$ protein expression. In two pairs of control and OGR1-overexpressing cell lines (pair #1; vector-PC3 and OGR1-PC3 and #2; EGFP-PC3 and OGR1-EGFP-PC3), OGR1 expression increased the expression of $G\alpha_{i1}$ protein, which was blocked by actinomycin D treatment, suggesting that the regulation was at the transcriptional level (Fig. 4, C).

To determine whether OGR1 affects cell proliferation in vitro, we conducted cell proliferation assays (both cell number count and MTT assays) in the presence (2% FBS) or absence of growth stimulation (0% FBS). Cells from different clones (vector-PC3 and OGR1-PC3) were incubated in serum-free media, and cell proliferation was determined after 24, 48, and 72 hours. Similar to what

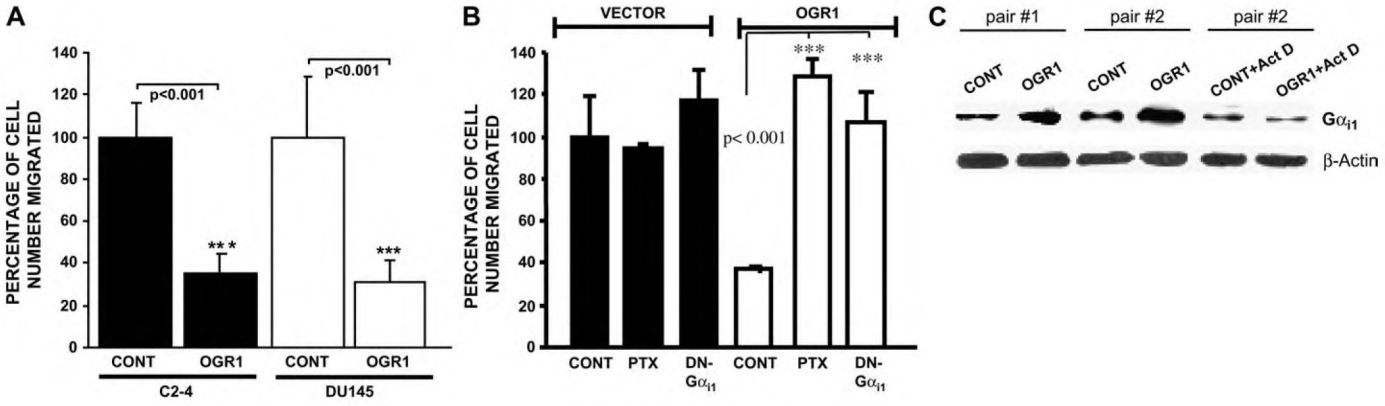

Fig. 4. The effect of ovarian cancer G protein–coupled receptor 1 (OGR1) on cell migration toward vitronectin in two other prostate cancer cell lines, C2-4 and DU145. **A**) C2-4 (**solid bars**) and DU145 (**open bars**) cells were transiently transfected with empty vector or a OGR1 plasmid and subjected to migration assay as in Fig. 3. **B**) Effects of treatment with pertussis toxin (PTX) (100 ng/mL) for 16 hours or transfection (1.5 μg of DNA per six-well plate) with a dominant-negative (DN–) form of G protein alpha–inhibitory subunit 1 ($G\alpha_{i1}$) on the inhibition of OGR1-PC3 cells migration. In **A** and **B**, mean (and 95% confidence intervals) percentages of migrated cells (result from four independent experiments in triplicate) are shown. P values (two-sided) were calculated using Student's t test. **C**) Immunoblotting was performed to test the effect of OGR1 on the expression of $G\alpha_{i1}$ protein level in two pairs of the control and the OGR1 cell lines in the absence (pair #1; vector-PC3 and OGR1-PC3 and #2; EGFP-PC3 and OGR1-EGFP-PC3) or in the presence of actinomycin D (pair#2 + ActD). The membrane was reprobed for β-actin to check for equal loading. One representative blot from three independent experiments is shown.

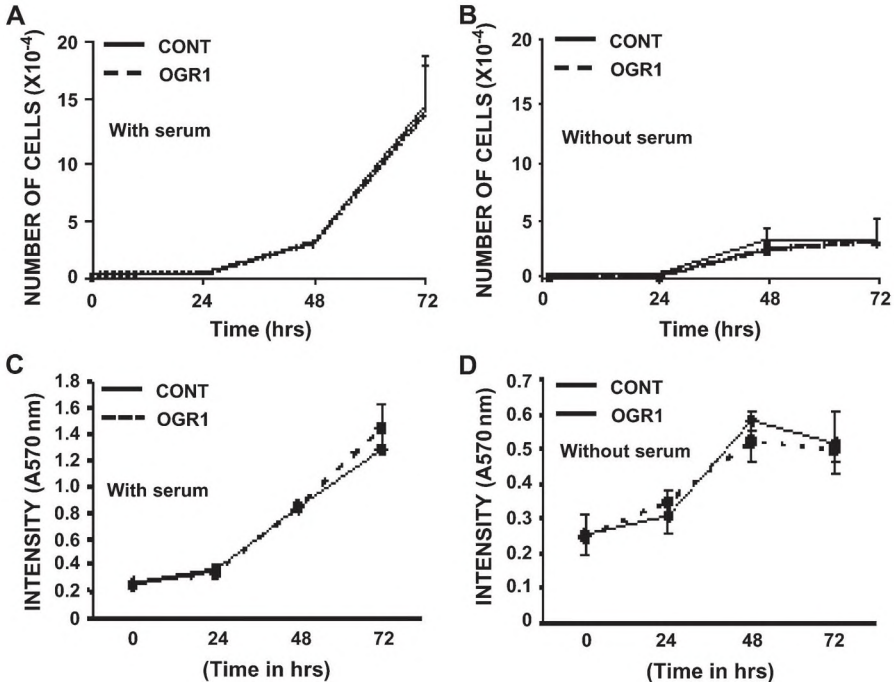

Fig. 5. Effects of ovarian cancer G protein–coupled receptor 1 (OGR1) expression on prostate cancer cell proliferation. In vitro cell proliferation assays were carried out in 48-well plates. Vector- or OGR1-PC3 cells (5×10^3) were cultured in RPMI with or without 2% fetal bovine serum. Cell proliferation was assessed by counting the cells (**A** and **B**) or by methylthiazolyldiphenyl-tetrazolium assays (**C** and **D**) at each time point. Mean (and 95% confidence intervals) numbers of cells counted by hemocytometer or absorbance intensity at 570 nm for one representative experiment performed in triplicate of more than ten independent experiments with similar results are shown.

was observed in vivo, OGR1 expression did not affect cell proliferation (Fig. 5). These results suggest that the in vitro behavior of the cells may reflect, at least in part, their in vivo properties and, thus, that some of their signaling mechanisms can be studied in vitro.

Secretion of an Antimigratory Factor Induced by OGR1

To test whether OGR1's inhibitory effect on cell migration is mediated by the secretion of a soluble factor, conditioned media was collected from vector-PC3 and OGR1-PC3 cells. Parental PC3 cells were then treated with this conditioned media and subjected to cell migration assays. Conditioned media from the OGR1-PC3 cells, but not vector-PC3 cells, inhibited the migration (mean percentage of cells migrated, 36.1% versus 100%, difference = 63.9%, 95% CI = 60.8% to 67.1%; $P<.001$) of parental PC3 cells (Fig. 6, A). The extent of this inhibition (60%–65%) is similar to that measured in the OGR1-PC3 cell migration assays (~70%). Collectively, these results suggest that a soluble factor(s) secreted into the conditioned media derived from OGR1-PC3 cells is responsible for the majority of the inhibitory effect on tumor cell migration (Fig. 3). To determine whether the conditioned media was required during cell migration or whether a short incubation time was sufficient for successful suppression, the parental cells

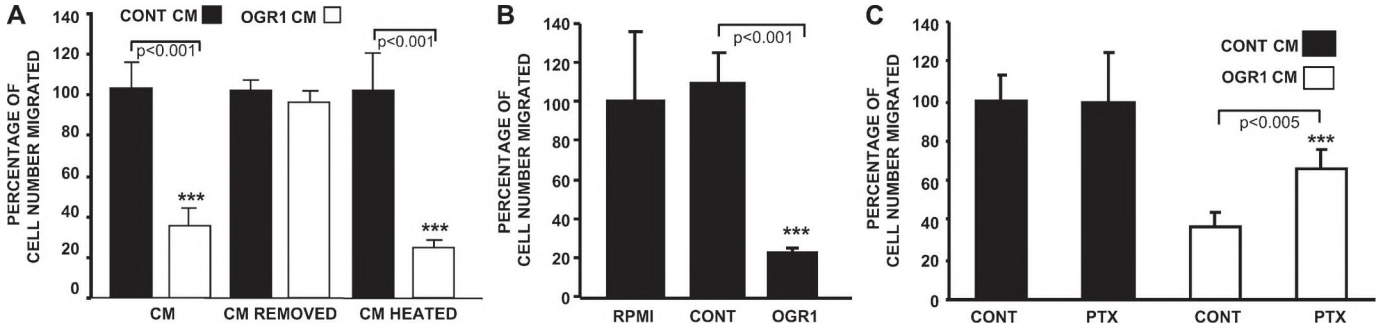

Fig. 6. Effects on the secretion of an antimigratory lipid factor in a G protein alpha–inhibitory subunit–dependent manner by ovarian cancer G protein–coupled receptor 1 (OGR1). **A**) Parental PC3 cells were incubated for 16 hours in serum-free RPMI medium, treated with trypsin–EDTA, washed twice with phosphate-buffered saline (PBS), and replated in conditioned media (CM) collected from either vector-PC3 or OGR1-PC3 cells for 30 minutes at 37 °C. Controls were treated as above but only washed twice with PBS after 30-minute incubation (CM removed). To test the effect of heated conditioned media on migration (CM heated), media from either vector-PC3 or OGR1-PC3 cells was preheated at 95 °C for 30 minutes and then incubated with parental PC3 cell before the cells were subjected to the migration assay. Mean (and 95% confidence intervals) percentage of cells migrated are shown for one representative of four independent experiments performed in triplicate (n = 3). **B**) The effect of lipid extracts prepared from serum-starved (RPMI) and vector-PC3 (CONT) or OGR1-PC3 (OGR1) cells on cell migration. Mean (and confidence intervals) percentage of cells migrated are shown for one representative of four independent experiments (performed in triplicate). **C**) Vector-PC3 (closed bars) and OGR1-PC3 (open bars) cells were either untreated (CONT) or pretreated with 100 ng/mL of pertussis toxin (PTX) for 12 hours. Cells were washed twice with PBS and incubated in serum-free RPMI for 12 hours. The conditioned media was then collected from PTX-pretreated cells and used to access its effect on parental PC3 cells migration. Mean (and 95% confidence intervals) percentage of cells migrated are shown for one representative of four independent experiments performed in triplicate. *P* values (two-sided) were calculated using Student's *t* test.

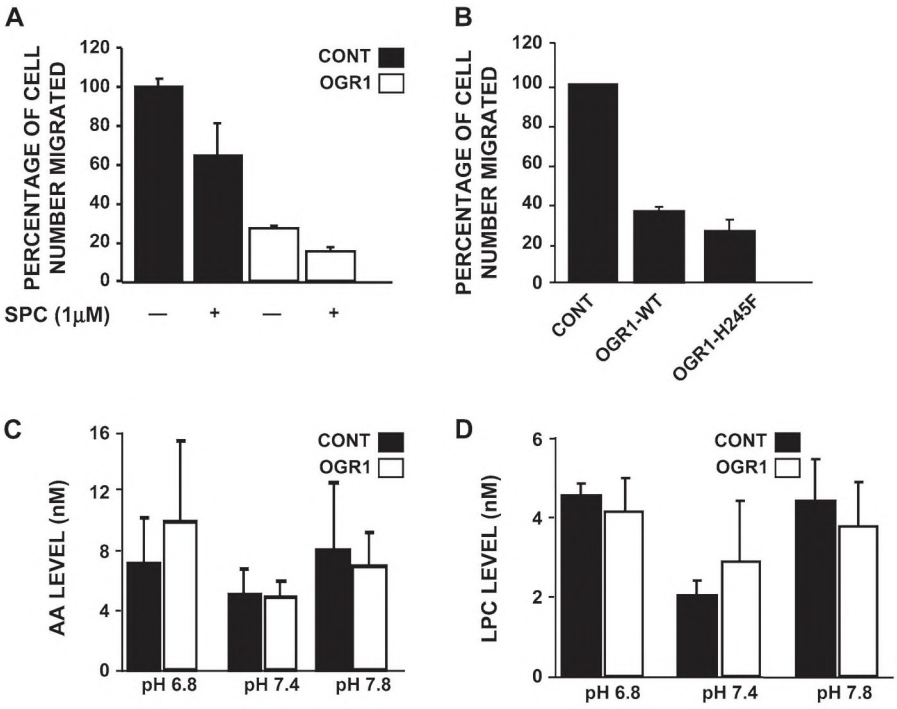

Fig. 7. The effect of sphingosylphosphorylcholine (SPC) and proton-sensing function of ovarian cancer G protein–coupled receptor 1 (OGR1) on cell **A**) Control- or OGR1-PC3 cells were incubated in serum-free RPMI for 12 hours and then untreated (–) or treated (+) with SPC (1 μM) for 30 minutes. Migration assays were then performed as described in Materials and Methods. **B**) PC3 cells were transiently transfected with 1.0–1.5 μg control vector (CONT), wild-type OGR1 (OGR1-WT), or proton-sensing OGR1 mutant DNA (OGR1-H245F). Cells were then incubated for 24 hours and then serum starved for an additional 12 hours before migration assays were performed. In **A** and **B**, mean (and 95% confidence intervals) percentage of cells migrated are shown for one representative of four independent experiments (performed in triplicate). **C** and **D**) Control- or OGR1-PC3 cells were incubated in physiologic salt solutions of different pHs for 90 minutes. Arachidonic acid (AA, **C**) and lysophosphatidylcholine (LPC, **D**) were extracted from the cell supernatants and quantified. Mean (and 95% confidence intervals) concentrations of AA ad LPC are shown for one representative of five independent experiments performed in triplicate. None of the comparisons between control versus OGR1 in Figs **C** and **D** were statistically significantly different (*P* values were all >.3, as determined using a [two-sided] Student's *t* test).

were pre-incubated in conditioned media for 30 minutes. The conditioned media was then removed by centrifugation, and the cells were resuspended in serum-free media before cell migration assays were performed. The inhibitory effect of the conditioned media was lost when the conditioned media was removed before the cell migration assay (Fig. 6, A), suggesting that a longer preincubation time or the presence of the inhibitory factor during the cell migration is necessary.

As the first step to identify the nature of this soluble factor, the conditioned media from OGR1-PC3 cells was heated to 95 °C for 30 minutes before migration assays were performed using parental PC3 cells. After heating, the conditioned media retained its antimigratory activity (Fig. 6, A), suggesting that a lipid factor is involved. However, because not all protein/peptide factors are heat labile, we cannot rule out the possible involvement of a heat-stable peptide factor in this process. To further investigate the nature of the factor, organic solvent extracts were prepared from conditioned media collected from OGR1-PC3, parental PC3, vector-PC3 cells, and serum-free media using chloroform/methanol extraction (2 : 1 vol/vol) and tested in migration assays as previously described. Parental PC3 cells that were pretreated with solvent extracts from OGR1-PC3–conditioned media migrated statistically significantly less (mean percentage of cells migrated = 25.0%, 95% CI = 22.7% to 27.3%, $P<.001$) than cells treated with solvent extracts from either the conditioned media from vector-PC3 (110%, 95% CI = 106.6% to 113.4%) or the serum-free media (100%, 95% CI = 63.8% to 136.2%). These results strongly suggest that the factor secreted in conditioned media derived from OGR1-PC3 cells is hydrophobic in nature.

To determine whether Gαi protein activation is involved in OGR1-induced secretion of this inhibitory factor, OGR1-PC3 cells were pretreated with PTX before conditioned media was collected. The effect of PTX-treated conditioned media from vector- and OGR1-PC3 cells on cell migration of parental PC3 cells was then compared. Although PTX did not affect migration induced by the conditioned media from the vector control cells, it reversed the inhibitory effect of the conditioned medium from OGR1-PC3 cells on cell migration (control versus OGR1: mean percentage of cells migrated, 98.7% versus 36.1%, difference = 62.6%, 95% CI = 50.61% to 74.57%; $P<.001$; Fig. 6, C), suggesting that Gαi protein activity is necessary for secretion of the inhibitory factor.

Because control cells (vector-PC3 or EGFP-PC3) did not secrete a stimulatory factor in their conditioned media (Fig. 6, B), it is likely that OGR1 expression enhances secretion of an inhibitory factor(s) instead of inhibiting secretion of a stimulatory factor. Thus, we expected to observe an increased amount of a hydrophobic factor in conditioned media from OGR1-PC3 cells compared with conditioned media from control cells. AA and LPC are the two major products of phospholipase A_2 (PLA_2) enzymes, and some of LPC's biologic activities may be mediated by the OGR1 subfamily of G protein–coupled receptors (14,33,34). However, we found that OGR1 expression did not increase secretion of either AA or LPC into the media at physiologic pH (7.4) (Fig. 7, C and D). Therefore, AA and LPC are unlikely to be involved in the inhibitory effect on migration. We also compared other positively or negatively charged ions in the range of 100–1000 kDa from the solvent extracts from the conditioned media from the control versus OGR1 samples using MS (data not shown). No molecular species were consistently increased in the lipids extracts from OGR1-PC3 cells.

Effects of SPC or OGR1's Proton-Sensing Activities on the OGR1 Antimigratory Phenotype

We and others have observed that OGR1 has constitutive activity (15,35,36). The in vivo and in vitro effects of OGR1 presented above were measured in the absence of exogenous stimuli (other than ECM proteins) and with a constant extracellular pH. Therefore,

the activities measured are likely to be mediated through the constitutive activation of OGR1.

To determine whether SPC influences the inhibitory effect of OGR1 on cell migration, we treated vector- and OGR1-PC3 cells with SPC (1 μM). SPC itself had an inhibitory effect on cell migration (Fig. 7, A) that was not affected by OGR1 expression. OGR1 has also been shown to have proton-sensing activity during inositol phosphate formation in the human embryonic kidney HEK293 and other cell types (20,25). In our experiments, the pH of the media was not changed, and therefore, it was unlikely that the proton-sensing activity of OGR1 is involved in OGR1's effect on cell migration. To further address this issue, we constructed an OGR1 mutant (OGR1-H245F) that has impaired proton-sensing ability (25). OGR1 H245F showed a similar inhibitory effect on cell migration as wild-type OGR1 (Fig. 7, B). Furthermore, we tested the effect of pH on AA and LPC secretion related to OGR1 expression and found that OGR1 expression did not affect AA and LPC production or secretion at any of the pHs tested (Fig. 7, C).

Discussion

Metastasis suppressor genes are a class of genes that reduce the metastatic propensity of cancer cell lines in vivo without affecting their tumorigenesis (2–4). In this article, we presented the following evidence to support the hypothesis that OGR1 is a novel metastasis suppressor gene in prostate cancer: 1) when OGR1 was overexpressed in PC3 cells, it suppressed tumor cell metastasis in an orthotopic mouse model of prostate cancer; 2) OGR1 did not affect primary tumor growth, as assessed by the size of the primary tumors and by BrdU incorporation assays; and 3) in vitro, OGR1 expression reduced cell migration, an important step in metastasis, without affecting cell proliferation. These data, together with a previous report showing that OGR1 expression is reduced in metastatic compared with primary prostatic tumors (24), support the hypothesis that OGR1 may have an important role in the metastasis of prostate cancer cells.

OGR1 has been shown to suppress tumor cell growth in ovarian cancer cells (36,37). When OGR1 was expressed fourfold to 10-fold above basal levels in PC3 cells, it did not affect cell growth. GPR4, a G protein–coupled receptor sharing more than 50% homology with OGR1, did not inhibit cell migration, suggesting a specific antimigratory role for OGR1. These results are consistent with an earlier report showing that GPR4 is oncogenic (38).

OGR1 has been shown to have a proton-sensing activity (17,25) that may be cell-type and signaling pathway specific (15,25). Because an acidic extracellular pH—a characteristic of the microenvironment of solid tumors—has been shown to enhance tumor metastatic potential (39), we have addressed the potential role of the proton-sensing ability of OGR1 in our assays. An OGR1 mutant (H245F) with minimal proton-sensing activity in inositol phosphate accumulation had the same effect as wild-type OGR1 on PC3 cell migration. Furthermore, OGR1 does not affect AA or LPC secretion at different pHs as compared with the control. In addition, OGR1's proton sensing activity is mediated by a $G_{\alpha q}$ protein (40). We have observed that a dominant-negative $G_{\alpha q}$ had no effect on OGR1's effect on cell migration (data not shown) and $G\alpha_{i1}$ mediates the OGRI's effect.

OGR1 and related G protein–coupled receptors may have dual functions for mediating signals from either lipids or protons (19,20,41). SPC, a bioactive lipid molecule, is able to modulate the proton-sensing activity of OGR1. In Chinese hamster ovary cells, SPC inhibits the acid-induced actions in a pH-dependent manner (42). We tested the effect of SPC on migration of PC3 cells and found that it was inhibitory. However, this inhibitory effect appeared to be independent of OGR1 expression. We cannot completely rule out that SPC may have an effect in vivo. These issues warrant further studies. Together, our data suggest that the in vitro effects of OGR1 described in this article are unlikely to be related to SPC or proton sensing and are constitutive in nature.

The mechanisms of OGR1's inhibitory effect on cell migration appeared to be related to $G\alpha_{i1}$ protein activation. G protein–coupled receptor constitutive activity can induce G protein activation. Interestingly, prostate cancer cells express relatively low levels of Gαi proteins, which may have an important regulatory role in cell proliferation and neoplastic transformation in these cells (43). In addition, immunoblot analysis shows that although the levels of β subunits of G proteins are maintained, those of α_s and α_i subunits are decreased 30%–40% after neoplastic transformation (43). We showed here that OGR1 expression increased $G\alpha_{i1}$ expression in PC3 cells and that this increase was likely to be at the transcriptional level.

G_i protein activation is involved in the stimulation of cell migration and in intracellular signaling through receptors for lysophosphatidic acid and sphingosine-1-phosphate (44–47). In contrast, G_i protein–mediated inhibition of cell migration is much less explored. Nevertheless, it has been shown that a G_i-mediated inhibition of cAMP accumulation is involved in the inhibitory effect of angiopeptin on the migration of vascular smooth muscle cells (48).

The present study has several limitations. Only one prostate cancer cell line was used in the in vivo models. OGR1's function in additional prostate cell lines should be tested in vivo. Bone metastasis is a major issue for human prostate cancer. The role of OGR1 in bone metastasis has not been assessed because we did not observe bone metastases in either the control or the OGR1 mice. This issue should be tested in different prostate cancer models. In addition, we have not identified the soluble factor that is responsible for the inhibitory effect of OGR1 on cell migration. It is possible that the migration inhibitory factor is present at lower concentrations and thus difficult to detect. It is also possible that the size or charge of the molecule is outside the detection range that we chose. Further studies are required to identify this factor. Nevertheless, our results do suggest that G_i protein activation is involved in the secretion of this OGR1-induced inhibitory factor.

Our results show that OGR1 suppresses prostate cancer metastasis without affecting primary tumor progression, suggesting that OGR1 is a novel metastasis suppressor gene for prostate cancer. Activation of G_{i1} and the secretion of a hydrophobic factor appear to be important for OGR1's antimetastatic action. Further investigation needs to be conducted to identify the soluble factor(s) involved in this process.

References

(1) Jemal A, Siegel R, Ward E, Murray T, Xu J, Smigal C, et al. Cancer statistics. CA Cancer J Clin 2006;56:106–30.

(2) Steeg PS, Ouatas T, Halverson D, Palmieri D, Salerno M. Metastasis suppressor genes: basic biology and potential clinical use. Clin Breast Cancer 2003;4:51–62.

(3) Steeg PS. Perspectives on classic article: metastasis suppressor genes. J Natl Cancer Inst 2004;96:E4.

(4) Shevde LA, Welch DR. Metastasis suppressor pathways—an evolving paradigm. Cancer Lett 2003;198:1–20.

(5) Yoshida BA, Sokoloff MM, Welch DR, Rinker-Schaeffer CW. Metastasis-suppressor genes: a review and perspective on an emerging field. J Natl Cancer Inst 2000;92:1717–30.

(6) Jiang Y, Berk M, Singh LS, Tan H, Yin L, Powell CT, et al. KiSS1 suppresses metastasis in human ovarian cancer via inhibition of protein kinase C alpha. Clin Exp Metastasis 2005;22:369–76.

(7) Steeg PS. Metastasis suppressors alter the signal transduction of cancer cells. Nat Rev Cancer 2003;3:55–63.

(8) Winter SF, Cooper AB, Greenberg NM. Models of metastatic prostate cancer: a transgenic perspective. Prostate Cancer Prostatic Dis 2003;6: 204–11.

(9) Kue PF, Taub JS, Harrington LB, Polakiewicz RD, Ullrich A, Daaka Y. Lysophosphatidic acid-regulated mitogenic ERK signaling in androgen-insensitive prostate cancer PC-3 cells. Int J Cancer 2002;102:572–9.

(10) Yowell CW, Daaka Y. G protein-coupled receptors provide survival signals in prostate cancer. Clin Prostate Cancer 2002;1:177–81.

(11) Kue PF, Daaka Y. Essential role for G proteins in prostate cancer cell growth and signaling. J Urol 2000;164:2162–7.

(12) Behan DP, Chalmers DT. The use of constitutively active receptors for drug discovery at the G protein-coupled receptor gene pool. Curr Opin Drug Discov Devel 2001;4:548–60.

(13) Xu Y, Casey G. Identification of human OGR1, a novel G protein-coupled receptor that maps to chromosome 14. Genomics 1996;35:397–402.

(14) Qiao J, Huang F, Naikawadi RP, Kim KS, Said T, Lum H. Lysophosphatidylcholine impairs endothelial barrier function through the G Protein-coupled receptor, GPR4. Am J Physiol Lung Cell Mol Physiol 2006;291:L91–101.

(15) Kim KS, Ren J, Jiang Y, Ebrahem Q, Tipps R, Cristina K, et al. GPR4 plays a critical role in endothelial cell function and mediates the effects of sphingosylphosphorylcholine. Faseb J 2005;19:819–21.

(16) Tosa N, Murakami M, Jia WY, Yokoyama M, Masunaga T, Iwabuchi C, et al. Critical function of T cell death-associated gene 8 in glucocorticoid-induced thymocyte apoptosis. Int Immunol 2003;15:741–9.

(17) Radu CG, Nijagal A, McLaughlin J, Wang L, Witte ON. Differential proton sensitivity of related G protein-coupled receptors T cell death-associated gene 8 and G2A expressed in immune cells. Proc Natl Acad Sci U S A 2005;102:1632–7.

(18) Im DS, Heise CE, Nguyen T, O'Dowd BF, Lynch KR. Identification of a molecular target of psychosine and its role in globoid cell formation. J Cell Biol 2001;153:429–34.

(19) Im DS. Two ligands for a GPCR, proton vs lysolipid. Acta Pharmacol Sin 2005;26:1435–41.

(20) Tomura H, Mogi C, Sato K, Okajima F. Proton-sensing and lysolipid-sensitive G-protein-coupled receptors: a novel type of multi-functional receptors. Cell Signal 2005;17:1466–76.

(21) Seifert R, Wenzel-Seifert K. Constitutive activity of G-protein-coupled receptors: cause of disease and common property of wild-type receptors. Naunyn Schmiedebergs Arch Pharmacol 2002;366:381–416.

(22) Nordhoff V, Gromoll J, Simoni M. Constitutively active mutations of G protein-coupled receptors: the case of the human luteinizing hormone and follicle-stimulating hormone receptors. Arch Med Res 1999;30:501–9.

(23) Boddy JL, Fox SB, Han C, Campo L, Turley H, Kanga S, et al. The androgen receptor is significantly associated with vascular endothelial growth factor and hypoxia sensing via hypoxia-inducible factors HIF-1a, HIF-2a, and the prolyl hydroxylases in human prostate cancer. Clin Cancer Res 2005;11:7658–63.

(24) LaTulippe E, Satagopan J, Smith A, Scher H, Scardino P, Reuter V, et al. Comprehensive gene expression analysis of prostate cancer reveals distinct transcriptional programs associated with metastatic disease. Cancer Res 2002;62:4499–506.

(25) Ludwig MG, Vanek M, Guerini D, Gasser JA, Jones CE, Junker U, et al. Proton-sensing G-protein-coupled receptors. Nature 2003;425:93–8.

(26) Bligh EG, Dyer WJ. A rapid method of total lipid extraction and purification. Can J Biochem Physiol 1959;37:911–7.

(27) Schmidt R, Coste O, Geisslinger G. LC-MS/MS-analysis of prostaglandin E2 and D2 in microdialysis samples of rats. J Chromatogr B Analyt Technol Biomed Life Sci 2005;826:188–97.

(28) Xiao YJ, Schwartz B, Washington M, Kennedy A, Webster K, Belinson J, et al. Electrospray ionization mass spectrometry analysis of lysophospholipids in human ascitic fluids: comparison of the lysophospholipid contents in malignant vs nonmalignant ascitic fluids. Anal Biochem 2001;290:302–13.

(29) Xiao Y, Chen Y, Kennedy AW, Belinson J, Xu Y. Evaluation of plasma lysophospholipids for diagnostic significance using electrospray ionization mass spectrometry (ESI-MS) analyses. Ann N Y Acad Sci 2000;905: 242–59.

(30) Shevrin DH, Kukreja SC, Ghosh L, Lad TE. Development of skeletal metastasis by human prostate cancer in athymic nude mice. Clin Exp Metastasis 1988;6:401–9.

(31) Bastide C, Bagnis C, Mannoni P, Hassoun J, Bladou F. A Nod Scid mouse model to study human prostate cancer. Prostate Cancer Prostatic Dis 2002;5: 311–5.

(32) Rembrink K, Romijn JC, van der Kwast TH, Rubben H, Schroder FH. Orthotopic implantation of human prostate cancer cell lines: a clinically relevant animal model for metastatic prostate cancer. Prostate 1997; 31:168–74.

(33) Lin P, Ye RD. The lysophospholipid receptor G2A activates a specific combination of G proteins and promotes apoptosis. J Biol Chem 2003; 278:14379–86.

(34) Radu CG, Yang LV, Riedinger M, Au M, Witte ON. T cell chemotaxis to lysophosphatidylcholine through the G2A receptor. Proc Natl Acad Sci U S A 2004;101:245–50.

(35) Bektas M, Barak LS, Jolly PS, Liu H, Lynch KR, Lacana E, et al. The G protein-coupled receptor GPR4 suppresses ERK activation in a ligand-independent manner. Biochemistry 2003;42:12181–91.

(36) Xu Y. Sphingosylphosphorylcholine and lysophosphatidylcholine: G protein-coupled receptors and receptor-mediated signal transduction. Biochim Biophys Acta 2002;1582:81–8.

(37) Xu Y, Xiao YJ, Zhu K, Baudhuin LM, Lu J, Hong G, et al. Unfolding the pathophysiological role of bioactive lysophospholipids. Curr Drug Targets Immune Endocr Metabol Disord 2003;3:23–32.

(38) Sin WC, Zhang Y, Zhong W, Adhikarakunnathu S, Powers S, Hoey T, et al. G protein-coupled receptors GPR4 and TDAG8 are oncogenic and overexpressed in human cancers. Oncogene 2004;23:6299–303.

(39) Kalliomaki T, Hill RP. Effects of tumour acidification with glucose+MIBG on the spontaneous metastatic potential of two murine cell lines. Br J Cancer 2004;90:1842–9.

(40) Iwai K, Koike M, Ohshima S, Miyatake K, Uchiyama Y, Saeki Y, et al. RGS18 acts as a negative regulator of osteoclastogenesis by modulating acid-sensing OGR1/NFAT signaling pathway. J Bone Miner Res 2007. [Jun 18 Epub ahead of print].

(41) Yang M, Mailhot G, Birnbaum MJ, Mackay CA, Mason-Savas A, Odgren PR. Expression of and role for ovarian cancer G-protein-coupled receptor 1 (OGR1) during osteoclastogenesis. J Biol Chem 2006;281:23598–605.

(42) Mogi C, Tomura H, Tobo M, Wang JQ, Damirin A, Kon J, et al. Sphingosylphosphorylcholine antagonizes proton-sensing ovarian cancer G-protein-coupled receptor 1 (OGR1)-mediated inositol phosphate production and cAMP accumulation. J Pharmacol Sci 2005;99:160–7.

(43) Garcia-Fernandez MO, Solano RM, Sanchez-Chapado M, Ruiz-Villaespesa A, Prieto JC, Carmena MJ. Low expression of Galpha protein subunits in human prostate cancer. J Urol 2001;166:2512–7.

(44) Panetti TS. Differential effects of sphingosine 1-phosphate and lysophosphatidic acid on endothelial cells. Biochim Biophys Acta 2002;1582: 190–6.

(45) Sugimoto N, Takuwa N, Yoshioka K, TakuwaRho-dependent Y. Rho kinase-independent inhibitory regulation of Rac and cell migration by LPA1 receptor in Gi-inactivated CHO cells. Exp Cell Res 2006;312:1899–908.

(46) Sugimoto N, Takuwa N, Okamoto H, Sakurada S, Takuwa Y. Inhibitory and stimulatory regulation of Rac and cell motility by the G12/13-Rho and Gi pathways integrated downstream of a single G protein-coupled sphingosine-1-phosphate receptor isoform. Mol Cell Biol 2003;23:1534–45.
(47) Liu F, Verin AD, Wang P, Day R, Wersto RP, Chrest FJ, et al. Differential regulation of sphingosine-1-phosphate- and VEGF-induced endothelial cell chemotaxis. Involvement of G(ialpha2)-linked Rho kinase activity. Am J Respir Cell Mol Biol 2001;24:711–9.
(48) Mooradian DL, Fernandes B, Diglio CA, Lester BR. Angiopeptin (BIM23014C) inhibits vascular smooth muscle cell migration in vitro through a G-protein-mediated pathway and is associated with inhibition of adenylyl cyclase and cyclic AMP accumulation. J Cardiovasc Pharmacol 1995;25:611–8.

Funding

National Institutes of Health (RO1 HL68804, RO1-CA89228 to Y. X.); Ralph C. Wilson, Sr. and Ralph C. Wilson, Jr. Medical Research Foundation grant (to Y. X.).

Notes

We are grateful for Dr Weiling Xu's help with the pathologic examination of slides. The sponsors had no role in the study design, data collection and analysis, interpretation of the results, the preparation of the manuscript, or the decision to submit the manuscript for publication.

Manuscript received April 21, 2007; revised June 25, 2007; accepted July 12, 2007.